PHILOSOPHICAL TRANSACTIONS OF THE ROYAL SOCIETY A MATHEMATICAL, PHYSICAL & ENGINEERING SCIENCES

Dynamics of the fire plume

G. Heskestad

Phil. Trans. R. Soc. Lond. A 1998 **356**, 2815-2833
doi: 10.1098/rsta.1998.0299

THE ROYAL SOCIETY

Dynamics of the fire plume

By G. Heskestad

Factory Mutual Research Corporation, Norwood, MA 02062, USA

The author reviews progress made in understanding and predicting the dynamics of fire plumes and suggests areas for further study. Turbulent plumes, axisymmetric in the mean, are considered, from the far-field, weakly buoyant to the near-flame, strongly buoyant elevations, into the flaming region. Developments are traced to the present capabilities of predicting plume diameter, temperature, and velocity practically down to the flame level, air entrainment rates along the entire plume, flame heights, flame pulsation frequencies, flame deflections in wind, and plume reach in density-stratified space. Some recent research relative to behaviour of mass fires (such as 'nuclear winter' fires) is reviewed, a combustion mode which appears to offer many research opportunities. Certain areas are identified which can benefit from future research. These include effects of in-depth combustion, the near-source region of fires with low flame-height-to-diameter ratio, flame pulsations, flame bending and trailing in wind, plume air entrainment in ambients not free of disturbances, and certain disparities between measurements of plumes from flaming sources and plumes from discharge of buoyant gas.

Keywords: fire plume; pool fire; mass fire

1. Introduction

Knowledge of fire plumes is important in solving many practical fire protection problems, for example, problems associated with fire detection, smoke filling rates of indoor spaces, fire venting, fire heating of structural elements of buildings, compartment fires, and indoor/outdoor thermal radiation hazards. Such knowledge can also be important in the design of fire suppression systems as related, for example, to the penetration of water drops to the base of a fire.

A fire plume may be defined as the motion generated by a source of buoyancy which exists by virtue of combustion and may incorporate an external source of momentum. The buoyancy source may be due to glowing or flaming combustion of a solid or liquid, with no external source of momentum, or due to gaseous, liquid, spray, or aerosol discharge from an opening at various mixes of mass flow and momentum. While the motion may be laminar or turbulent, or both, this paper deals with turbulent motion which, by far, predominates in fire situations. Only non-premixed combustion is considered, the most common in fire. When an initial momentum is present, it is assumed that it is aligned with and directed against the gravity vector. Discussion is further limited to fire plumes which are axisymmetric in the mean.

One finds that the common candle has a laminar flame plume and a subsequent laminar, non-reacting plume up to a height of perhaps 200–300 mm, where transition to turbulence may take place. The author has experimented with small vessels of heptane on substrates of water and found that the flame-tip regions of the plumes exhibited turbulence when the diameter of the vessel reached approximately 30 mm,

with a heat release rate of approximately 300 W and a flame height of about 120 mm. This size, then, is representative of the minimum source strength considered in this paper. The nature of the turbulent, non-reacting plume is not found to vary appreciably from the scale of small laboratory fires to large industrial fires (Heskestad 1981).

Evidence indicates (Heskestad 1986) that in order for the entire flame plume to be considered fully turbulent (in the sense that insignificant changes appear to occur in the gross motion of the flame plume for larger fire sources), a minimum fire diameter of approximately 300 mm may be needed (at least for buoyancy dominated fires with heat release rates greater than 10 kW).

Knowledge of the behaviour of fire plumes is mostly based on observations and dimensional analysis, complemented by analytical models. Numerical analysis of turbulent fires is now beginning to show promise (Cox & Kumar 1987; Holen *et al*. 1991), based on the k–ε turbulence model (Launder & Spalding 1972) and a combustion model by Magnussen & Hjertager (1976). Another approach is offered by Baum *et al*. (1994) in which the fire driven flow is decomposed into large-scale convective and small-scale combustion components, requiring no empirical turbulence models. However, acceptable reliability of predictions deep in the combustion region is still to be demonstrated. This paper will not dwell any further on numerical approaches.

Section 2 focuses on plumes in a uniform environment, considering, first, point sources of buoyancy, then flaming area sources, and finally area sources of small ratios of heat release rate per unit area to the square root of diameter, which are characteristic of mass fires and produce interesting fire behaviour. Section 3 deals with fire plumes in winds, with a new analysis of data on flame bending and 'trailing' collected in the 1960s. Finally, in § 4, we discuss plumes in density stratified spaces based on classical, as well as new research.

2. Plumes in quiescent and uniformly dense space

(*a*) *Point source*

The first plume theories (Schmidt 1941; Rouse *et al*. 1952; Morton *et al*. 1956) assumed (i) turbulent flow; (ii) a point source of buoyancy; (iii) variations of density in the field of motion which are small compared to the ambient density; and (iv) dynamic similarity of the mean and turbulent motion at all elevations. Morton *et al*. (1956) developed an integral formulation which employed an entrainment coefficient, α, defined as the ratio of inflow velocity at the edge of the plume to the vertical velocity within the plume. Assuming 'top-hat' profiles, these authors derived the following expressions, in the case of uniform ambient fluid, for variations with elevation above the point source, z, of the mean radius to the edge of the plume, b, the mean vertical velocity in the plume, u, and the mean density deficiency, $\Delta\rho$ (where $g(c_pT_a\rho_a)^{-1}Q_c$, has been substituted for the buoyancy flux $b^2ug(\rho_a-\rho)/\rho_a$, using the ideal gas law, Q_c being the convective heat flux in the plume):

$$b = \frac{6\alpha}{5}z, \tag{2.1}$$

$$u = \frac{5}{6}\left(\frac{9}{10\pi\alpha^2}\right)^{1/3} g^{1/3}(c_p\rho_aT_a)^{-1/3}Q_c^{1/3}z^{-1/3}, \tag{2.2}$$

$$\frac{\Delta\rho}{\rho_\mathrm{a}} = \frac{5}{6}\left(\frac{9\pi^2\alpha^4}{10}\right)^{-1/3} g^{-1/3}(c_p\rho_\mathrm{a}T_\mathrm{a})^{-2/3}Q_\mathrm{c}^{2/3}z^{-5/3}. \tag{2.3}$$

Equations (2.1)–(2.3) are the weak plume (small density deficiency) relations for a point source. For other than a point source, a virtual source location or virtual origin, z_v, is introduced and z in the equations replaced by $z - z_\mathrm{v}$. In addition, to accommodate large density deficiencies, which exist in fire plumes, Morton (1965) replaced $\Delta\rho/\rho_\mathrm{a}$ in (2.3) with $\Delta\rho/\rho$ ($= \Delta T/T_\mathrm{a}$ using the ideal gas law) and added the factor $(\rho_\mathrm{a}/\rho)^{1/2}$ ($= (T/T_\mathrm{a})^{1/2}$ using the ideal gas law) on the right side of (2.1).

Measurements in fire plumes above the flames have to a large extent supported the theory, with the following results and numerical coefficients (Heskestad 1984):

$$b_{\Delta T} = 0.12(T_0/T_\mathrm{a})^{1/2}(z - z_\mathrm{v}), \tag{2.4}$$

$$\Delta T_0 = 9.1[T_\mathrm{a}/(gc_p^2\rho_\mathrm{a}^2)]^{1/3}Q_\mathrm{c}^{2/3}(z - z_\mathrm{v})^{-5/3}, \tag{2.5}$$

$$u_0 = 3.4[g/(c_p\rho_\mathrm{a}T_\mathrm{a})]^{1/3}Q_\mathrm{c}^{1/3}(z - z_\mathrm{v})^{-1/3}. \tag{2.6}$$

Here, $b_{\Delta T}$ is the plume radius to the point where the mean temperature rise is $\frac{1}{2}\Delta T_0$; ΔT_0 and T_0 are the mean excess temperature and mean temperature, respectively, on the centreline, and u_0 is the mean centreline velocity. These equations are known as the strong plume relations. The numerical coefficients were determined from data-sets for which the locations of the virtual origin, z_v, were established (Kung & Stavrianidis 1983).

For comparison, turbulent plumes generated by buoyant, non-reacting vertical discharges from nozzles may be considered. Results have been presented which are said to belong to a downstream, buoyancy dominated regime, i.e. essentially free of effects of the Froude number of the discharge. George *et al.* (1977) established the set of coefficients 0.104, 9.1, and 3.4, the same as in equations (2.4)–(2.6) except for the smaller value, 0.104, compared to 0.12. Papanicolaou & List (1988) found the coefficients 0.09, 14.3, and 3.9. Recent experiments by Shabbir & George (1994) indicated the set 0.10, 9.4, and 3.4, while those of Dai *et al.* (1994) indicated 0.08, 12.6, and 'not measured'. The initial Froude numbers of the discharges, $\rho_\mathrm{a}u^2/(\Delta\rho gD)$, ranged from 0.2 to 61.

In addition to the temperature radius, $b_{\Delta T}$, a velocity radius, b_u, can be defined as the radius to the point where the gas velocity is one-half the centreline value. According to Heskestad (1988), ratios of velocity radius to temperature radius have been reported from fire and plume experiments which range from 0.86 (Rouse *et al.* 1952) to 1.5 (Cox & Chitty 1980). Most reliable are believed to be the measurements of George *et al.* (1977) and Shabbir & George (1994) with ratios of 1.08 and 1.07, respectively.

The shapes of the mean velocity and mean temperature rise profiles appear to be almost Gaussian (Shabbir & George 1994), although there is no theoretical basis for this distribution.

(*b*) *Flaming area sources*

The strong-plume relations, (2.4)–(2.6), are also valid for the non-reacting plume above an area source provided the virtual origin can be located, which leads to consideration of the flames, their relationship to the non-reacting plume, and other issues of interest such as air entrainment and shedding of vortex structures.

PHILOSOPHICAL TRANSACTIONS OF THE ROYAL SOCIETY A MATHEMATICAL, PHYSICAL & ENGINEERING SCIENCES

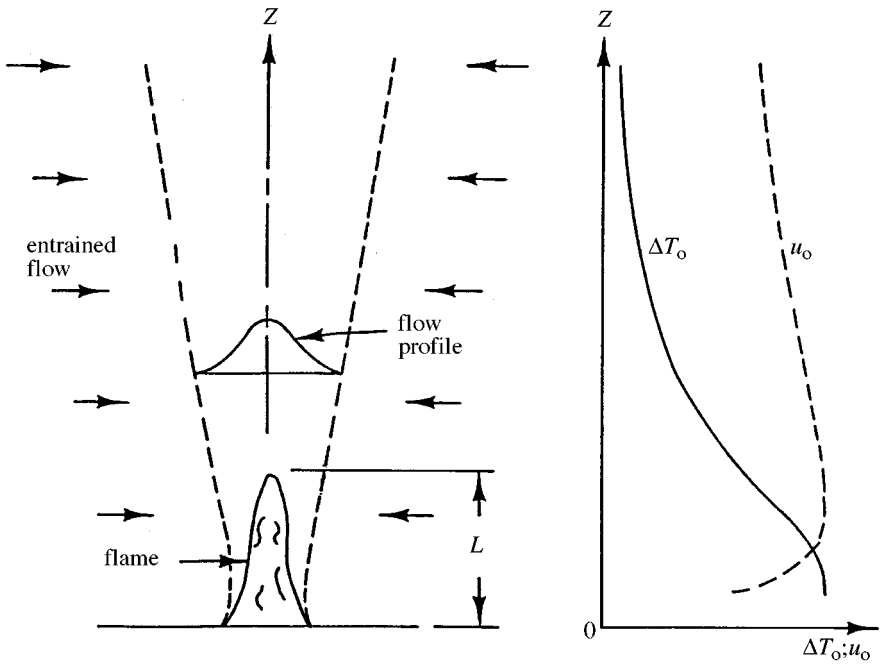

Figure 1. Features of a pool fire. z is the height above the pool surface; ΔT_0 and u_0 are temperature rise and gas velocity, respectively, on the plume axis.

Figure 1 illustrates a fire plume originating on a flaming area source (horizontal, flaming area sources are often referred to as pool fires). Combustible volatiles generated from the fuel bed by heat from the flames mix with the surrounding air and form a diffusion flame of mean flame height L. Surrounding the flames is a boundary (dashed lines) which confines the combustion products and across which air is entrained. This boundary is instantaneously very sharp, highly convoluted, sometimes penetrated by the combustion interface, and easily discernible in smoky fires. The flow profile could be the time-averaged temperature rise above the ambient temperature, the concentration of a gas such as carbon dioxide, or the axial velocity in the fire plume.

Figure 1 (right) suggests how the temperature rise on the centreline, ΔT_0, and the velocity on the centreline, u_0, might behave, based on observations (McCaffrey 1979; Cox & Chitty 1980; Heskestad 1981; Kung & Stavrianidis 1983; Gengembre *et al.* 1984). In this example with a relatively tall flame, the mean temperatures are nearly constant in the lower portion of the flame and begin to decrease in the intermittent, upper portion of the flame as the combustion reactions trail off and air is entrained from the surroundings to cool the flow. The centreline mean velocities, u_0, tend to peak slightly below the mean flame height. If the combustible is porous and supports internal combustion, there may not be as pronounced a fall-off in the gas velocity toward the combustible as suggested in the figure (Heskestad 1981).

A pioneering paper by Thomas (1963) focused attention on, and made early contributions to, several of the topics discussed below, paving the way for progress made to date.

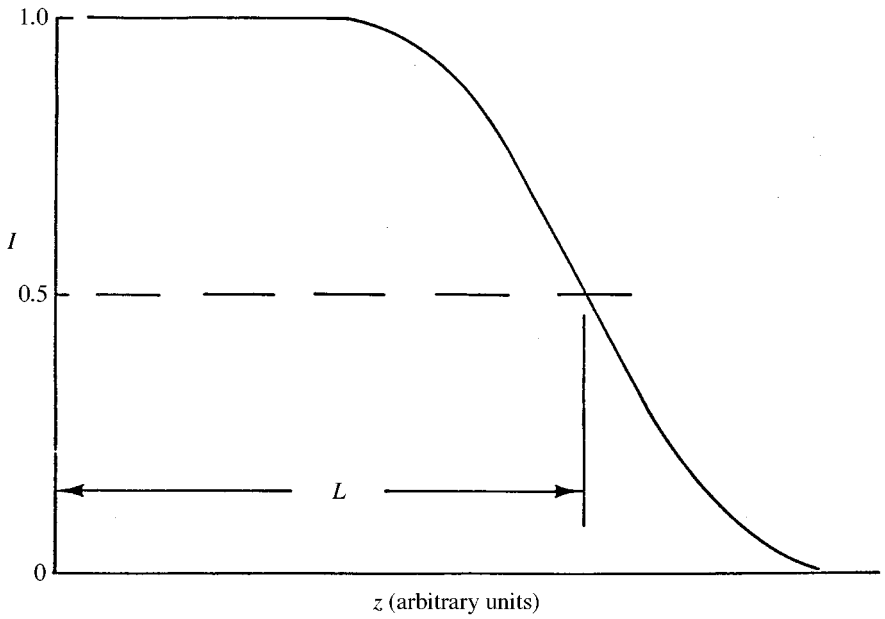

Figure 2. Mean flame height, L, defined from intermittency (I) distribution (Zukoski *et al.* 1985).

(i) *Flame height*

The visible flames mark the combustion reaction zone. Figure 2 clarifies the mean flame height in terms of the flame intermittency (Zukoski *et al.* 1985), $I(z)$, which is the fraction of time that at least part of the flame lies above the elevation, z. The mean flame height, L, is the distance above the fire source where the intermittency has decreased to 0.5. The flame height marks the level where the combustion reactions are essentially complete and the inert plume can be considered to begin. Tamanini (1983) has investigated the manner in which combustion approaches completion with respect to height in diffusion flames.

Several expressions for mean flame height have been advanced based on correlations of experimental data, which have been reviewed by McCaffrey (1988). A general correlation has been proposed by Heskestad (1983), based on the assumption that the flames will extend to the height where sufficient air has been entrained from the surroundings to complete the combustion reactions (assuming fast combustion kinetics) and, further, built on a capability of predicting maximum gas velocities associated with buoyancy-controlled turbulent diffusion flames (Heskestad 1981). Non-dimensional flame height is expressed as a function of N.

$$L/D = f(N), \tag{2.7}$$

where D is the fire diameter and N is the non-dimensional group:

$$N = \left[\frac{c_p T_\mathrm{a}}{(g\rho_\mathrm{a}^2(\Delta H_\mathrm{c}/r)^3}\right]\frac{Q^2}{D^5}. \tag{2.8}$$

Available data for many combustibles and fire diameters were correlated well according to (Heskestad 1983):

$$L/D = -1.02 + 15.6N^{1/5}. \tag{2.9}$$

Alternatively, (2.9) can be written:

$$L/D = -1.02 + AQ^{2/5}/D, \tag{2.10}$$

where the value $A = 0.235\ \mathrm{m\ kW^{-2/5}}$ is representative of a large number of gaseous and liquid fuels under normal atmospheric conditions.

The flame-height relation (2.9) does not include fire sources with substantial in-depth combustion, such as very openly constructed wood cribs (Heskestad 1981). The range in N for which this equation has been found to be valid extends from a high limit of 10^5 (Heskestad 1981), associated with flames beginning to show effects of discharge momentum, to near the lower limit, 1.195×10^{-6}, where the calculated value of L/D becomes negative (Heskestad 1991). In § 2 *c*, the lower limit is associated with entry into a flaming regime characteristic of mass fires. One cannot rule out effects of the density of the fuel gas, relative to the ambient density, on the flame-height ratio, but such effects are yet to be reported. There is some evidence (Heskestad 1995) that there are no significant effects of fire size (or more properly, Reynolds number) as long as at least the flame tip region is turbulent, as in the case of the 30 mm diameter heptane source mentioned in § 1.

Measurements by Hasemi & Tokunaga (1984*a*) for square and round gas burners in the range of N from 1.6×10^{-2} to 7.9×10^{-5} show little effect of the burner shape when, for the square burners, D is taken as the diameter of a circular burner of equal area. Subsequent measurements of Hasemi & Nishihata (1988) have indicated tendencies to slightly higher flame-height ratios than circular burner data when N becomes smaller than 1.0×10^{-5}.

Investigations by Orloff (1981) and Orloff & de Ris (1982) revealed that the height of a peripheral rim or lip above the surface of a circular pool fire affects the burning rate and flame shape, but has little effect on the flame height (except through Q).

Other geometric effects on flames have attracted attention. Without further comment, these include interactions with ceilings (Gross 1989), interactions with walls and corners (Hasemi & Tokunaga 1984*b*), and interaction/merging of proximate flames (Sugawa & Takahashi 1993; Thomas *et al*. 1965).

(ii) *Virtual origin*

Applications of the relations (2.4)–(2.6) require knowledge of the location of the virtual origin, z_v, which has been investigated by several authors reviewed by Heskestad (1988).

Heskestad (1983) assumes that, except for absolute scales, the shapes of the mean velocity and temperature profiles at the mean flame height are invariant, which leads to the hypothesis,

$$z_\mathrm{v} = L - Eb_{uL}, \tag{2.11}$$

where z_v is the elevation of the virtual origin above the top of the combustible, L is the mean flame height above the top of the combustible, b_{uL} is the radius at the mean flame height, and E is a non-dimensional constant. A Froude number characteristic

of the local plume flow is employed, needed here and generally useful for calculating plume velocities, u_0:

$$\xi = \left[\frac{T_a^{2/5}(c_p\rho_a)^{1/5}}{g^{2/5}}\right]\frac{u_0}{(\Delta T_0 Q_c)^{1/5}}, \tag{2.12}$$

which is found to be invariant at a value of $\xi = 2.2$ in the non-reacting plume and well into the intermittent flaming region (Heskestad 1981). A relation for b_{uL} is obtained with the aid of the convective-heat flux integral over the plume cross-section at the mean flame height, together with (2.12):

$$b_{uL} = [2\pi\beta\xi(c_p\rho_a)^{4/5}T_a^{3/5}g^{2/5}]^{-1/2}\frac{T_{0L}^{1/2}Q_c^{2/5}}{\Delta T_{0L}^{3/5}}, \tag{2.13}$$

where β is a constant, non-dimensional integral, evaluated from measurements as $\beta = 0.41$. Combining (2.9) with (2.11)–(2.13), there results,

$$z_v/D = -1.02 + FQ^{2/5}/D, \tag{2.14}$$

where the coefficient F is dependent on the environment (c_p, T_a, ρ_a, g) and the combustible $(\Delta H_c/r)$. Using centreline temperature data from a number of investigations, the value $F = 0.083\ \mathrm{m\ kW^{-2/5}}$ was determined by Heskestad (1983) for normal atmospheric conditions (and common values of $\Delta H_c/r$ near $3000\ \mathrm{kJ\ kg^{-1}}$). Here we see that the virtual origin can be above (positive z_v) or below (negative z_v) the surface of the combustible.

Since the flame-height relation (2.9), used in the derivation of (2.14), becomes inaccurate when there is substantial in-depth combustion, the expression for the virtual origin, (2.14), also becomes inaccurate for such fire sources.

(iii) *Transition, flames to non-reacting plume*

The strong-plume relations, (2.4)–(2.6), cease to be valid at and below the mean flame height. However, it is possible to generate a plot of mean centreline plume temperatures for the entire plume, including the flames. Note that $Q_c^{2/3}(z - z_v)^{-5/3}$ in (2.5) can be written $[(z - z_v)/Q_c^{2/5}]^{-5/3}$, which suggests the type plot in figure 3 of ΔT_0 versus $(z - z_v)/Q_c^{2/5}$, a type first introduced by McCaffrey (1979) and later refined by Kung & Stavrianidis (1983) who introduced the virtual origin, z_v. The sloping straight line in the figure corresponds to (2.5) at normal atmospheric conditions. The abscissa value $0.175\ \mathrm{m\ kW^{-2/5}}$ corresponds to the mean flame height according to (2.10) and (2.14) (with $A = 0.235$ and $F = 0.083\ \mathrm{m\ kW^{-2/5}}$); an associated mean temperature rise of about 500 K is indicated. Deep in the flames the mean temperature rise reaches approximately 900 K. Values of mean temperature rise as high as 1000 K have been observed by Gregory *et al.* (1989) in large, $9 \times 18\ \mathrm{m^2}$ pool fires; the data in figure 3 are associated with fire diameters up to 2.5 m (Kung & Stavrianidis 1983).

Fires with low flame-height-to-diameter ratios have not been investigated extensively and may require special consideration with respect to near-source temperatures and velocities. For example, such fires will tend to have negative values of z_v, which may push the minimum possible abscissa values in figure 3 so high that the maximum temperatures seen in the figure may not be realized. Some evidence exists for such behaviour (Heskestad 1988). There is also uncertainty associated with assuming that

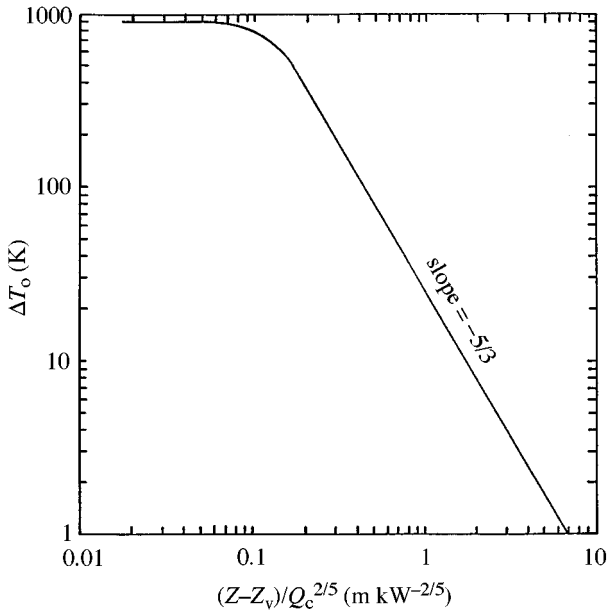

Figure 3. Temperature rise on the plume centreline for normal atmospheric conditions (Heskestad 1984), in form attributable to McCaffrey (1979) and Kung & Stavrianidis (1983).

ξ in (2.12) remains constant down to the flame level in these cases, although ξ may still remain constant down to the height where the maximum gas velocity occurs.

(iv) *Air entrainment*

The mass flow at a particular elevation in a fire plume is nearly completely attributable to air entrained by the plume at lower elevations. The mass flow contributed by the fire source itself is insignificant in comparison, on the order of 1% of the mass flow rate at the level of the flame tip (Heskestad 1986).

For a weak plume, the mass flow rate at a cross-section is written:

$$\dot{m}_{\mathrm{ent}} = G\rho_{\mathrm{a}} u_0 b_u^2, \tag{2.15}$$

where G is a non-dimensional constant. With the aid of (2.6) and the equivalent of (2.4) written for b_u (setting $T_0/T_{\mathrm{a}} = 1$ because of the weak plume assumption), (2.15) becomes

$$\dot{m}_{\mathrm{ent}} = G\left[\frac{g\rho_{\mathrm{a}}^2}{c_p T_{\mathrm{a}}}\right]^{1/3} Q_{\mathrm{c}}^{1/3}(z - z_{\mathrm{v}})^{5/3}. \tag{2.16}$$

Cetegen *et al.* (1982, 1984) concluded that (2.16) also applies to strongly buoyant plumes. From extensive entrained-flow measurements for natural-gas burners of several diameters, these authors proposed a coefficient $G = 0.21$. However, the plume flow rates at large heights were somewhat overpredicted and those at low heights, approaching the flames, underpredicted.

Heskestad (1986) reconsidered the entrainment problem, assuming self-preserving density deficiency profiles instead of self-preserving excess temperature profiles as

traditionally assumed, with the result:

$$\dot{m}_{\mathrm{ent}} = G\left[\frac{g\rho_{\mathrm{a}}^2}{c_p T_{\mathrm{a}}}\right]^{1/3} Q_{\mathrm{c}}^{1/3}(z - z_{\mathrm{v}})^{5/3}\left[1 + \frac{JQ_{\mathrm{c}}^{2/3}}{(g^{1/2}c_p\rho_{\mathrm{a}}T_{\mathrm{a}})^{2/3}(z - z_{\mathrm{v}})^{5/3}}\right]. \qquad (2.17)$$

This equation, with $G = 0.196$ and $J = 2.9$, was found to represent measurements very well over the entire non-reacting plume above the flames. Mass flow rates at levels below the flame tip were found to increase linearly with height for fire diameters of 0.3 m and greater, where the flames are substantially turbulent, from zero (essentially) at the fire base to the flame-tip value given by (2.17) evaluated at $z = L$ (for normal atmospheric conditions and $\Delta H_{\mathrm{c}}/r = 3000$, the flame tip value is $\dot{m}_{\mathrm{ent},L}$ (kg s^{-1}) $= 0.0059Q_{\mathrm{c}}$ (kW)).

Cetegen *et al.* (1982, 1984), whose data provided the main support for equation (2.17), have pointed out that their fire plumes were produced in as quiet an atmosphere as could be maintained in their laboratory. They reported that small ambient disturbances could provide 20–50% increases in the measured plume mass flows. Clearly, there is a need for further research.

Other noteworthy contributions to the study of entrained flows in fire plumes include those of Yih (1952), Thomas *et al.* (1963, 1965), McCaffrey (1979), Hinkley (1986), Delichatsios (1987), Zukoski (1994), and Zhou & Gore (1995).

(v) *Turbulence and pulsations*

Knowledge about the turbulence structure in plumes is available from measurements in buoyant plumes of hot air discharged vertically upward.

Recently, Shabbir & George (1994) reported measurements of terms appearing in the mean energy and momentum equations and also presented a review of earlier turbulence measurements. Most instructive are measurements on the centreline for turbulence intensities of temperature and velocity in the buoyancy dominated regime. For intensities of axial velocity fluctuations, u'/u_0, the authors quote values from four different sources, including their own, in the range 0.25–0.33, with an average of 0.28. The associated intensities of temperature fluctuations, $T'/\Delta T_0$, are quoted in the range 0.36–0.42, with an average of 0.39.

Turbulence measurements, using a laser-Doppler anemometer, have been made by Gengembre *et al.* (1984) on the axis above a 0.30 m diameter propane burner. In the plume region above the flames, down to the level of maximum mean axial velocity just below the flame tip, the intensity of the axial velocity fluctuations were measured at $u'/u_0 = 0.33$ (heat release rates ranging from 16 to 38 kW), which is at the high end of the range for a non-reacting plume source quoted above from Shabbir & George (1994).

The turbulent velocity fluctuations measured by Gengembre *et al.* (1984) above flaming fire sources may have included contributions traceable to pulsations of the flames. Such pulsations have been the subject of a number of investigations, tracing at least back to Rasbash *et al.* (1956) and reviewed in conjunction with a recent study reported by Cetegen & Ahmed (1993). Byram & Nelson (1970) describe the pulsation cycle as starting 'with the expansion of the flames near the base of the fire and is followed by a sudden collapse of these flames toward the centre of the fire. A flame bulge then travels upward to the flame tip in an even, wavelike motion. Expansion of the lower part of the flames starts the cycle again.'

PHILOSOPHICAL TRANSACTIONS OF THE ROYAL SOCIETY A MATHEMATICAL, PHYSICAL & ENGINEERING SCIENCES

Cetegen & Ahmed (1993) summarize the published data on the pulsation frequency in a single plot for burner diameters ranging from about 0.03 to 20 m. They propose the simple curve fit:

$$f\ (\mathrm{Hz}) = 1.5(D\ (\mathrm{m}))^{-1/2}. \tag{2.18}$$

(Previous investigators have proposed similar relations.) However, the data-scatter is large; measured frequencies near a given fire diameter differ by a factor as large as two.

In view of the success of the scaling concepts developed for flame height, the following non-dimensional, functional relation might be tested on the available data:

$$fD/u_{0L} = f(N), \tag{2.19}$$

where u_{0L}, the mean axial velocity at the flame tip, is represented by the velocity derived from (2.12) setting T_0 equal to the flame tip value.

(*c*) *Mass fires*

The smooth curve in figure 4, taken from Heskestad (1991), is the empirical fit to experimental flame-height data according to (2.9). Data from the low-N region are presented from measurements by Zukoski *et al*. (1980/81), Wood *et al*. (1971) and Heskestad (1991). Wood *et al*. (1971) reported that coherent flaming behaviour changed to distributed flamelets when L/D became smaller than 0.5 ($\log_{10} L/D = -0.30$), which occurs near $N = 10^{-5}$ ($\log_{10} N = -5$).

The data trend in figure 4 seems to be that L/D approaches zero at a limiting value of N near 10^{-6}, which is unphysical. This trend led Heskestad (1991) to speculate that continuous flaming would not be possible on a homogeneous fuel below a limiting value of N near 10^{-6}, interpreted as a lean flammability limit, and this hypothesis was tested in a fire experiment. The experiment involved igniting a 7.3 m × 7.3 m, flat, horizontal array of wood-fibre boards impregnated with a controlled amount of heptane as ignitor. Photographs from the experiment are presented in figure 5. As the fire decayed from an initial state of relatively high intensity, figure 5*a*, the flaming pattern developed non-flaming areas as seen in figure 5*b*, *c*. With the aid of auxiliary experiments it was possible to show that the extinguished areas in the flaming pattern were due to dynamic effects of the fire and not attributable to local burn-out of the fuel bed.

The value of N for which L/D becomes negative according to (2.9) is 1.195×10^{-6}. For normal atmospheric conditions and common fuel properties, this limit can be converted to, using (2.8):

$$(\dot{q}''/D^{1/2})_{\mathrm{limit}} = 53\ \mathrm{kW\ m^{-5/2}}. \tag{2.20}$$

For heat release rates per unit area of 2500 kW m^{-2}, which can be considered representative of high heat-release rate liquids such as heptane and gasoline, the predicted fire diameter where continuous flaming breaks up is calculated as 2230 m. For 5000 kW m^{-2}, representative of LNG spills, the break-up diameter is predicted to be 8900 m.

'Mass fires' are usually taken to mean fires of diameters that may reach to tens of kilometres in projected nuclear winter scenarios, most often incorporating multiple fuel beds. An understanding of such fires would be very important and the field is ripe for experimental research. Numerical solutions will be very demanding of computer power and are not expected to be feasible for some time.

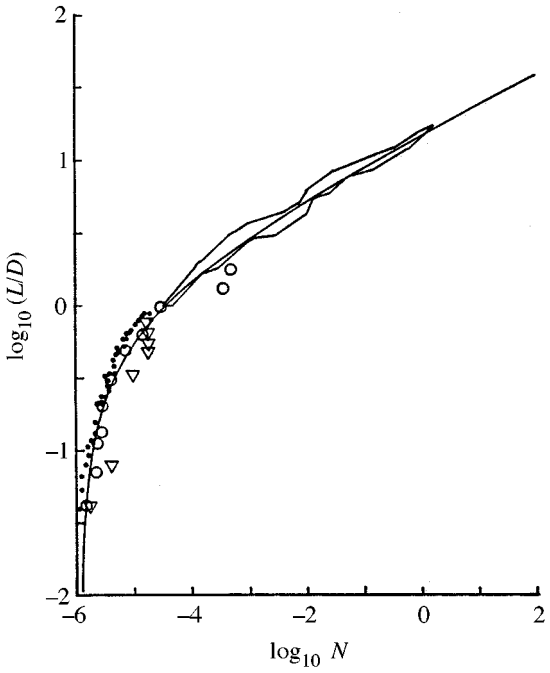

Figure 4. Flame-height data in low-N region compared to empirical curve fit in (2.9), including stretched envelope containing 80 data points (natural gas) from Zukoski *et al.* (1980/81), open circles (acetone) and triangles (methanol) from Wood *et al.* (1971), and solid circles (propane) from Heskestad (1991).

3. Windblown flames

Many fire scenarios may involve a wind field, either in exterior locations, or in the draft of makeup air inside a room ventilated through a door.

The main effect of the wind is to bend or deflect the flames away from the vertical. Another effect, observed in wind tunnel studies (Welker & Sliepcevich 1965), is 'flame trailing', in which the flames trail off the burner along the floor in the downwind direction for a significant distance. Flame trailing was thought to be associated primarily with fuel vapours of greater density (higher molecular weight) than air, as was the case with all of the various liquid fuels used in the experiments.

The rather extensive wind tunnel experiments of Welker & Sliepcevich (1965) were conducted with five different flammable liquids (acetone, benzene, cyclohexane, n-hexane, methyl alcohol) in vessels of the following approximate diameters: 0.10 m, 0.21 m, 0.31 m, 0.47 m, and 0.60 m. For different wind velocities, measurements were taken of fuel burning rate, flame angle from the vertical, θ, flame length, L, and flame trailing distance. The authors developed correlations for both flame bending and trailing.

Later, large-scale data on flame bending were obtained by Attalah & Raj (1974), involving square pools of LNG having equivalent diameters (diameter of a circle having the same area as a square surface) of 2.1 m, 6.9 m, and 27.5 m. Their flame deflection angles were not consistent with the correlation of Welker & Sliepcevich (1965).

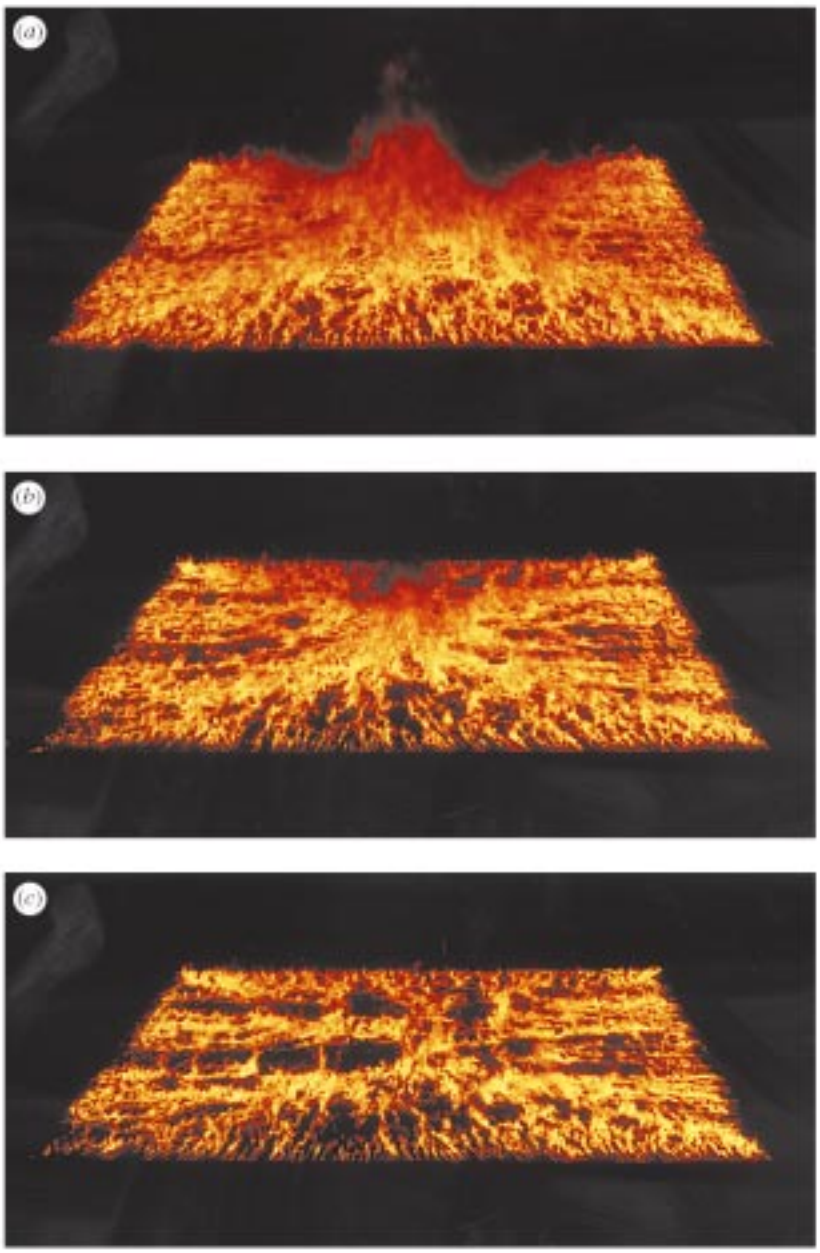

Figure 5. Decaying fire on 7.3 m × 7.3 m assembly of wood-fibre board resting on floor. (*a*) Fire decays as heptane burns off (near 18 s from ignition). (*b*) Further decay and first indications of break-up in flaming pattern (near 21 s). (*c*) Definite patchiness in flaming pattern (near 26 s).

The scaling principles embodied in the flame-height correlation (2.9) suggest plotting the flame deflection angle as a function of the ratio of wind speed, u_{w}, to the mean axial velocity at the flame tip, u_{0L}, and recognizing that the parameter N (or L/D for quiescent conditions according to (2.9)) may be of some importance.

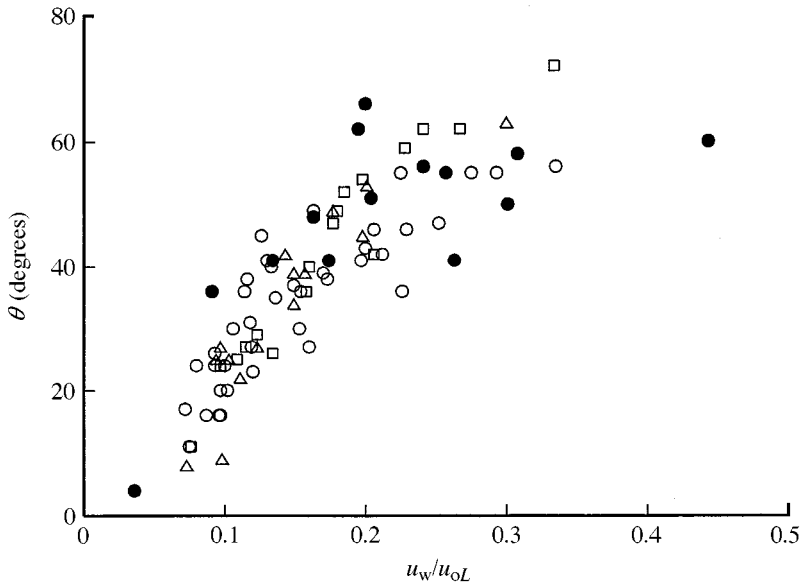

Figure 6. Flame deflection in wind. Open symbols are from small-scale experiments by Welker & Sliepcevich (1965) and solid circles are from large-scale LNG burns by Attalah & Raj (1974). ○, $(L/D)_{\mathrm{ref}} = 3.7$–$4.7$; △, $(L/D)_{\mathrm{ref}} = 2.5$–$2.9$; □, $(L/D)_{\mathrm{ref}} = 1.1$–$1.5$; ●, $(L/D)_{\mathrm{ref}} = 2.4$–$3.8$.

Figure 6 is such a plot for both the small-scale wind tunnel data (Welker & Sliepcevich 1965) involving many fuels and pool diameters, and the large-scale LNG burns reported by Attalah & Raj (1974). The correlation of the data is quite good. The effect of the parameter, $(L/D)_{\mathrm{ref}}$, which is the value of L/D according to (2.9), does not appear to be significant, within the scatter.

The effect of the wind on flame length (at constant $(L/D)_{\mathrm{ref}}$) in the data of Welker & Sliepcevich (1965) was minor in the range of abscissa values of figure 6, i.e. up to $u_{\mathrm{w}}/u_{0L} = 0.3$. In subsequent experiments extended to larger wind velocities (Huffman *et al*. 1967), some effect of wind on flame length can be observed. At a velocity ratio $u_{\mathrm{w}}/u_{0L} = 1.0$, flame lengths appear to have been approximately 30% greater than under quiescent conditions.

4. Plumes in density-stratified space

Morton *et al*. (1956) have considered turbulent plumes of a point source of buoyancy in a stably stratified atmosphere where the ambient density decreases linearly with height, equivalent to a linear increase in temperature with height at constant ambient pressure. This work has, until recently, mainly been applied to geophysical problems. Turner (1986) draws attention to the following examples: thermal plumes from large fires in the atmosphere, hot gas and ash emitted from erupting volcanoes, and less dense magma injected into stratified magma chambers. Less esoteric applications may be found for air and water pollution problems. Murgai & Emmons (1960) have calculated the natural convection over a fire of arbitrary size in an atmosphere with arbitrary lapse-rate variation.

Heskestad (1989) has interpreted the work of Morton *et al*. (1956) to building fires, with emphasis on the maximum height achieved by plumes in temperature-

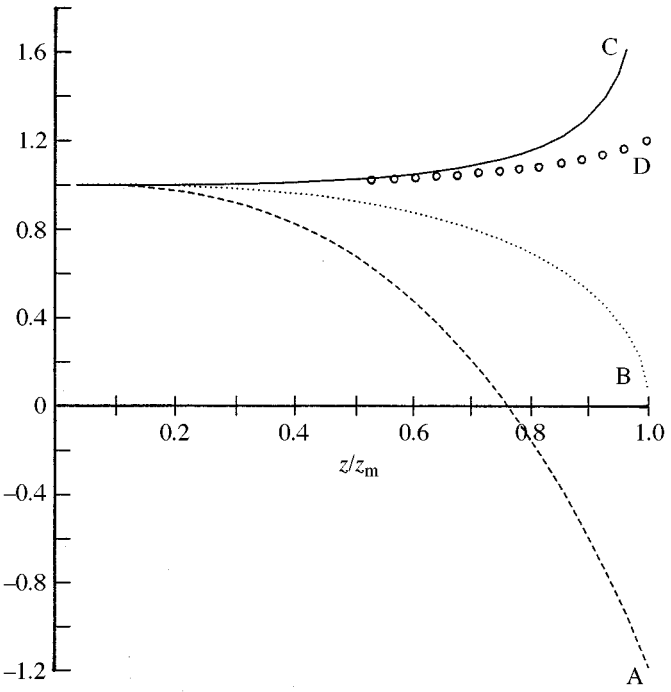

Figure 7. Theoretical behaviour of centreline plume variables in linearly temperature-stratified ambients. From Heskestad (1989), traceable to Morton *et al*. (1956). Curve A: ratio of temperature rises (stratified versus unstratified). Curve B: ratio of axial velocities. Curve C: ratio of plume radii. Curve D: ratio of volumetric species concentrations.

stratified spaces and deviations in theoretical plume behaviour from that in a uniform environment. For example, an expression for maximum plume rise becomes, in the translation,

$$z_m = 3.79\left[\frac{T_{a1}}{g(\rho_{a1}c_p)^2}\right]^{1/8} Q_c^{1/4}\left[\frac{dT_a}{dz}\right]^{-3/8}, \tag{4.1}$$

where dT_a/dz is the ambient temperature gradient, T_{a1} and ρ_{a1} are the ambient temperature and density, respectively, at the level of the source. The constant 3.79 traces to experiments by Morton *et al*. (1956) using dyed light liquid injected into a density-stratified salt solution. Figure 7, taken from Heskestad (1989), shows the ratio on the plume centreline of stratified value versus unstratified value for various plume variables: temperature rise relative to the pre-existing value at each level (curve A), axial velocity (B), plume radius (C), and (the implied) volume concentration of a combustion species (D). The ratios are plotted as functions of the fraction of maximum elevation achieved by the plume, z/z_m. By definition, the stratified velocity (B) decreases to zero at $z/z_m = 1$. The stratified temperature rise (A) becomes negative below the maximum reach. The stratified plume radius grows rapidly in approach to the maximum plume reach. However, there is little effect of the stratification on the centreline variation of concentration of a combustion species.

In a recent paper, Heskestad (1995) reports on experiments with turbulent thermal plumes (from small flaming heat sources) in variously temperature-stratified spaces.

For linear stratifications, he found quite good agreement with the results in figure 7 for temperature rise (A) and volume concentration (D) up to the theoretical plume reach, but the experimental values needed an incremental height, roughly equal to 25% of the theoretical plume reach, to return to zero.

The maximum plume reach can be interpreted in terms of a critical ambient temperature rise from the source level to an elevated observation plane, just strong enough to prevent plume fluid from penetrating the plane. Heskestad (1995) reports that this critical temperature rise is surprisingly insensitive to the shape of the stratification profile. For one nonlinear stratification profile, where one-half of the ambient temperature rise to the observation plane occurred higher than 59% of the elevation of the observation plane above the source, the critical ambient temperature rise could hardly be distinguished from that for a linear profile. For a more strongly nonlinear profile, where one-half of the ambient temperature rise to the observation plane occurred higher than 75% of the elevation of the observation plane above the source, the critical ambient temperature rise was 12% greater than that for the linear profile. The critical ambient temperature rise for a linear profile is 7.4 times the centreline temperature rise at the level of the observation plane which results from a fire source in a uniform environment.

In addition to the results referred to above, Heskestad (1995) also presents detailed spatial distributions of temperature rise and concentration of carbon dioxide. For a linear temperature stratification, regions above approximately two-thirds of the distance from the fire source to the reach of the plume showed a temperature decrease (relative to locally pre-existing values) in the laterally spreading cloud of plume gases.

5. Conclusions

1. Numerical models applied to turbulent fire plumes are showing promise, but still have to prove themselves, especially in the combustion region.

2. Plume theories, originally developed for weak, non-reacting plumes from point sources, have been improved and generalized over several decades so that predictions can now be made of plume diameter, temperature, and velocity, practically down to the flame level of area sources of fire. Near-source regions of fires with low flame-height-to-diameter ratios require further research.

3. Original theory for plumes in density-stratified space has been supported by experiments and, furthermore, predictive capabilities have been extended beyond the scope of the original theory.

4. Laboratory experiments with discharge of buoyant gases (including heated air) into ambient air have provided information on the turbulent velocity and density fields. However, these experiments have resulted in narrower plumes in the buoyancy dominated regime than observed above flaming area sources, which has not been explained.

5. The flaming region of circular area sources of common experience is well mapped, including flame heights, air entrainment, flame pulsations, and response to wind. However, additional research is needed to delineate effects of in-depth combustion on flame height and virtual origin, to improve correlations

for flame pulsations and wind effects such as flame bending and trailing, and to clarify effects of ambient disturbances on air entrainment into plumes.

6. The flaming regions of area fires of the kind expected in mass fires, including 'nuclear winter' fires, are only beginning to be understood and should offer many research opportunities.

Symbols

b	mean radius to edge of plume
$b_{\Delta T}$	mean plume radius to point where $T/T_0 = 0.5$
b_u	mean plume radius to point where $u/u_0 = 0.5$
c_p	specific heat at constant pressure
D	diameter
f	frequency
g	acceleration due to gravity
ΔH_c	heat of combustion per unit mass
I	intermittency
L	mean flame height
$\dot{m}_{ent}$	entrained mass flow rate
N	non-dimensional parameter defined in (2.8)
Q	total heat release rate
Q_c	convective heat release rate
q''	heat release rate per unit area
r	mass stoichiometric ratio, air to fuel
T	mean temperature
T'	RMS temperature fluctuations
ΔT	$T - T_a$
u	mean vertical velocity
u_w	wind speed
u'	RMS vertical velocity fluctuations
z	elevation above combustible or buoyancy source
z_m	maximum theoretical plume reach above source
z_v	height of virtual origin above combustible
α	entrainment coefficient
β	non-dimensional parameter
θ	flame deflection from vertical
ξ	non-dimensional parameter defined in (2.12)
ρ	mean density
$\Delta\rho$	$\rho_a - \rho$

Subscripts

a	ambient value
L	at mean flame height
0	on centreline
1	at source level

References

Attalah, S. & Raj, P. K. 1974 Radiation from LNG fires. In *Interim Report on Phase H Work*. American Gas Association Project IS-3.1 LNG Safety Program.

Baum, H. R., McGrattan, H. R. & Rehm, R. G. 1994 Mathematical modelling and computer simulation of fire phenomena. In *Fire Safety Science—Proc. Fourth Int. Symp.* (ed. T. Kashiwagi), pp. 185–193. International Association for Fire Safety Science.

Byram, G. M. & Nelson Jr, R. M. 1970 The modelling of pulsating fires. *Fire Technol.* **6**, 102–110.

Cetegen, B. M. & Ahmed, T. A. 1993 Experiments on the periodic instability of buoyant plumes and pool fires. *Combust. Flame* **23**, 157–184.

Cetegen, B. M., Zukoski, E. E. & Kubota, T. 1982 Entrainment and flame geometry of fire plumes. Report G8-9014, California Institute of Technology, Daniel and Florence Guggenheim Jet Propulsion Center.

Cetegen, B. M., Zukoski, E. E. & Kubota, T. 1984 Entrainment in the near and far field of fire plumes. *Combust. Sci. Technol.* **39**, 305–331.

Cox, G. & Chitty, R. 1980 A study of the deterministic properties of unbounded fire plumes. *Combust. Flame* **39**, 191–209.

Cox, G. & Kumar, S. 1987 Field modelling of fire in forced ventilated enclosure. *Combust. Sci. Technol.* **52**, 7–23.

Dai, Z., Tseng, L.-K. & Faeth, G. M. 1994 Structure of round, fully developed, buoyant turbulent plumes. *J. Heat Transfer* **116**, 409–417.

Delichatsios, M. A. 1987 Air entrainment into buoyant jet flames and pool fires. *Combust. Flame* **70**, 33–46.

Gengembre, E., Cambray, P., Karmed, D. & Bellet, J. C. 1984 Turbulent diffusion flames with large buoyancy effects. *Combust. Sci. Technol.* **41**, 55–67.

George, W. K., Alpert, R. L. & Tamanini, F. 1977 Turbulence measurements in an axisymmetric buoyant plume. *Int. J. Heat Mass Transfer* **20**, 1145–1154.

Gregory, J. J., Keltner, N. R. & Mata Jr, R. 1989 Thermal measurements in large pool fires. *J. Heat Transfer* **111**, 446–454.

Gross, D. 1989 Measurement of flame lengths under ceilings. *Fire Safety Jl* **15**, 31–44.

Hasemi, Y. & Nishihata, M. 1988 Deterministic properties of turbulent diffusion flames from low Q^* fires. In *9th Joint Panel Meeting of the USJNR Panel on Fire Research and Safety* (ed. N. H. Jason & B. A. Housten), pp. 41–49. US Department of Commerce, National Bureau of Standards.

Hasemi, Y. & Tokunaga, T. 1984*a* Flame geometry effects on the buoyant plumes from turbulent diffusion flames. *Fire Sci. Technol.* **4**, 15–26.

Hasemi, Y. & Tokunaga, T. 1984*b* Some experimental aspects of turbulent diffusion flames and buoyant plumes from fire sources against a wall and in a corner of walls. *Combust. Sci. Technol.* **40**, 1–17.

Heskestad, G. 1981 Peak gas velocities and flame heights of buoyancy-controlled turbulent diffusion flames. In *Eighteenth Symp. (Int.) on Combustion*, pp. 951–960. Pittsburgh: The Combustion Institute.

Heskestad, G. 1983 Luminous heights of turbulent diffusion flames. *Fire Safety Jl* **5**, 103–108.

Heskestad, G. 1984 Engineering relations for fire plumes. *Fire Safety Jl* **7**, 25–32.

Heskestad, G. 1986 Fire plume air entrainment according to two competing assumptions. In *Twenty-first Symp. (Int.) on Combustion*, pp. 111–120. Pittsburgh: The Combustion Institute.

Heskestad, G. 1988 Fire plumes. In *SFPE handbook on fire protection engineering* (ed. P. J. DiNenno), pp. 1-107–1-115. Boston: Society of Fire Protection Engineers.

Heskestad, G. 1989 Note on maximum rise of fire plumes in temperature-stratified ambients. *Fire Safety Jl* **15**, 271–276.

Heskestad, G. 1991 A reduced-scale mass fire experiment. *Combust. Flame* **83**, 293–301.

Heskestad, G. 1995 Fire plume behavior in temperature stratified ambients. *Combust. Sci. Technol.* **106**, 207–228.

Hinkley, P. L. 1986 Rates of 'production' of hot gas in roof venting experiments. *Fire Safety Jl* **10**, 57–65.

Holen, J., Brostrom, M. & Magnussen, B. F. 1991 Finite difference calculation of pool fires. In *Twenty-Third Symp. (Int.) on Combustion*, pp. 1677–1683. Pittsburgh: The Combustion Institute.

Huffman, K. G., Welker, J. R. & Sliepcevich, C. M. 1967 Wind and interaction effects on free-burning fires. Technical Report No. 1441-3, NBS Contract CST 1142 with University of Oklahoma.

Kung, H. C. & Stavrianidis, P. 1983 Buoyant plumes of large-scale pool fires. In *Nineteenth Symp. (Int.) on Combustion*, pp. 905–912. Pittsburgh: The Combustion Institute.

Launder, B. E. & Spalding, D. B. 1972 *Mathematical models of turbulence*. London: Academic.

McCaffrey, B. J. 1979 Purely buoyant diffusion flames: some experimental results. NBSIR 79-1910, National Bureau of Standards, Washington, DC.

McCaffrey, B. J. 1988 Flame height. In *SFPE handbook of fire protection engineering* (ed. P. J. DiNenno), pp. 1-298–1-305. Boston: Society of Fire Protection Engineers.

Magnussen, B. F. & Hjertager, B. H. 1976 On mathematical modeling of turbulent combustion with special emphasis on soot formation and combustion. In *Sixteenth Symp. (Int.) on Combustion*, pp. 719–729. Pittsburgh: The Combustion Institute.

Morton, B. R. 1965 Modeling of fire plumes. In *Tenth Symp. (Int.) on Combustion*, pp. 973–982. Pittsburgh: The Combustion Institute.

Morton, B. R., Taylor, G. I. & Turner, J. S. 1956 Turbulent gravitational convection from maintained and instantaneous sources. *Proc. R. Soc. Lond.* A **234**, 1–23.

Murgai, M. P. & Emmons, H. V. 1960 Natural convection above fires. *J. Fluid Mech.* **8**, 611–624.

Orloff, L. 1981 Simplified radiation modeling of pool fires. In *Eighteenth Symp. (Int.) on Combustion*, pp. 549–561. Pittsburgh: The Combustion Institute.

Orloff, L. & de Ris, J. 1982 Froude modeling of pool fires. In *Nineteenth Symp. (Int.) on Combustion*, pp. 885–895. Pittsburgh: The Combustion Institute.

Papanicolaou, P. N. & List, E. J. 1988 Investigation of round vertical turbulent buoyant jets. *J. Fluid Mech.* **195**, 341–391.

Rasbash, D. J., Rogowski, Z. W. & Stark, G. W. V. 1956 Properties of fires of liquids. *Fuel* **35**, 94–107.

Rouse, H., Yih, C. S. & Humphreys, H. W. 1952 Gravitational convection from a boundary source. *Tellus* **4**, 201–210.

Schmidt, W. 1941 Turbulente Ausbreitung eines Stromes erhitzer Luft. *Z. Angew. Math. Mech.* **21**, 265–278, 351–363.

Shabbir, A. & George, W. K. 1994 Experiments on a round turbulent buoyant plume. *J. Fluid Mech.* **275**, 1–32.

Sugawa, 0. & Takahashi, W. 1993 Flame height behavior from multi-fire sources. *Fire Mater.* **17**, 111–117.

Tamanini, F. 1983 Direct measurements of the longitudinal variation of burning rate and product yield in turbulent diffusion flames. *Combust. Flame* **51**, 231–243.

Thomas, P. H. 1963 The size of flames from natural fires. In *Ninth Symp. (Int.) on Combustion*, pp. 844–859. Pittsburgh: The Combustion Institute.

Thomas, P. H., Hinkley, P. L., Theobald, C. R. & Sims, D. L. 1963 Investigation into the flow of hot gases in roof venting. Fire Technical Paper No. 7. Joint Fire Research Organization, London: HMSO.

PHILOSOPHICAL TRANSACTIONS OF THE ROYAL SOCIETY A MATHEMATICAL, PHYSICAL & ENGINEERING SCIENCES

Thomas, P. H., Baldwin, R. & Heselden, A. J. M. 1965 Buoyant diffusion flames: some measurements of air entrainment, heat transfer, and flame merging. In *Tenth Symp. (Int.) on Combustion*, pp. 983–996. Pittsburgh: The Combustion Institute.

Turner, J. S. 1986 Turbulent entrainment: the development of the entrainment assumption, and its application to geophysical flows. *J. Fluid Mech.* **173**, 431–471.

Welker, J. R. & Sliepcevich, C. M. 1965 The effect of wind on flames. Technical Report No. 2, NBS Contract CST 1142 with University of Oklahoma.

Wood, B. D., Blackshear Jr, P. L. & Eckert, E. R. 1971 Mass fire model: an experimental study of the heat transfer to liquid fuel burning from a sand-filled pan burner. *Combust. Sci. Technol.* **4**, 113–129.

Yih, C.-S. 1952 Free convection due to a point source of heat. In *Proc. 1st US Natn. Cong. Appl. Mech.*, pp. 941–947.

Zhou, X. C. & Gore, J. P. 1995 Air entrainment flow field induced by a pool fire. *Combust. Flame* **100**, 52–60.

Zukoski, E. E. 1994 Mass flux in fire plumes. In *Fire Safety Science—Proc. Fourth Int. Symp.* (ed. T. Kashiwagi), pp. 137–147. International Association of Fire Safety Science.

Zukoski, E. E., Kubota, T. & Cetegen, B. 1980/81 Entrainment in fire plumes. *Fire Safeiy Jl* **3**, 107–121.

Zukoski, E. E., Cetegen, B. M. & Kubota, T. 1985 Visible structure of buoyant diffusion flames. In *Twentieth Symp. (Int.) on Combustion*, pp. 361–366. Pittsburgh: The Combustion Institute.

PHILOSOPHICAL TRANSACTIONS OF THE ROYAL SOCIETY A MATHEMATICAL, PHYSICAL & ENGINEERING SCIENCES